Electronic Supporting Information (ESI)

Unravelling the influence of human serum environment on drug release from nanoformulations with polyethylene glycol shell

Anjali Saini,[†a] Laura McKay,[†a] Fei Rui Long,[a] Morteza Mahmoudi,[b] Hojatollah Vali,[c] and Ashok Kakkar[a]*

[a] Department of Chemistry, McGill University, 801 Sherbrooke St. West, Montreal, Quebec H3A 0B8, Canada.

[b] Department of Radiology, College of Human Medicine, Michigan State University, East Lansing, MI USA; Precision Health Program, Michigan State University, East Lansing, MI, USA.

[c] Department of Anatomy & Cell Biology, McGill University, 3460 University Street, Montreal, Quebec, H3A 0C7 Canada.

*Corresponding author: ashok.kakkar@mcgill.ca

† These authors contributed equally.

Table of Contents

1. Materials and Methods

1.1 Materials and Instrumentation

Purified water was obtained from a Millipore Milli-Q® (MQ) system. ε-caprolactone monomer (99%, ACROS Organics) was distilled over CaH_2 before use, copper(I) bromide (CuBr, 98%, Sigma-Aldrich), 18-crown-6 (99%, Sigma-Aldrich), curcumin (CUR, ≥65%, Sigma-Aldrich), 3,5-dihydroxy benzyl (99%, Sigma-Aldrich), ethylenediaminetetraacetic acid disodium salt dihydrate (EDTA) (99.0-101.0%, Sigma-Aldrich), magnesium sulphate anhydrous ($MgSO_4$, Fisher Chemical) N,N,N′,N″,N″-pentamethyl diethylenetriamine (PMDETA) (99%, Sigma-Aldrich), poly(ethylene glycol) methyl ether ($mPEG_{2000}$-OH, 2000 g/mol, TCI Chemicals), sodium azide (NaN_3, ≥99.5%, Sigma-Aldrich), p-toluene sulfonyl chloride (≥98%, Sigma-Aldrich), triethylamine (ACP chemicals), and tin(II) 2-ethylhexanoate ($Sn(Oct)_2$, 92.5-100.0%, Sigma-Aldrich), Human serum (Sigma, H6914) were used as received. Serum concentration of HSA determined by UV-Vis (ε_{280} = 36,500 $M^{-1}cm^{-1}$) to be 1065 μM.[1] Anhydrous solvents were passed through activated alumina in an MBraun solvent purification system. Dialysis membranes (Spectrum ™ Spectra / Por ™, MWCO: 3.5 kDa) were purchased from Fisher Scientific. Solvents for NMR analysis were purchased from Cambridge Isotope Laboratories and used as received.
NMR characterizations were performed on a Bruker AVIIIHD 500 MHz NMR Spectrometer. Gel permeation chromatography (GPC) was performed on a Waters Breeze GPC system with HPLC grade THF as the mobile phase. Particle size measurements utilized a Brookhaven90Plus Particle Size Analyser equipped with a 40 mW red diode laser. A Thermo Scientific Talos F200X with a Ceta 16 M 4k x 4k CMOS camera was employed for transmission electron microscopy (TEM). UV-Vis absorption spectra were recorded on a Agilent Cary 50 spectrophotometer and fluorescence measurements were carried out on a Agilent Cary Eclipse spectrophotometer with slit widths fixed at 5 nm.

1.2 Methods

1.2.1 Preparation of blank and CUR loaded polymeric micelles

In the preparation of CUR loaded micelles, AB_2 or AB copolymers (5.0mg) were dissolved in 1.0 mL of HPLC-grade acetone. Subsequently, 1.0 mL of a 0.5 mg/mL stock solution of CUR in HPLC grade acetone (2.0 mg CUR in 4.0 mL acetone) was transferred to the copolymer solution. For blank (cargo-free) micelles, the selected copolymer (5.0 mg) was directly dissolved in 2.0 mL of HPLC acetone. The final organic solution ([Copolymer] = 2.5 mg/mL) was manually added to 2.0 mL of Milli-Q water (stirring at 400 rpm) at a rate of 1 drop per 5 seconds. The acetone evaporated while the mixture was continuously stirred in the dark overnight. After confirmation by mass of full acetone evaporation, the solutions were passed twice through 0.22 μm polyvinylidene fluoride (hydrophilic) syringe filters and used promptly.
The following equations were used to calculate encapsulation efficiency (EE %) and loading capacity (LC %):

$$EE\ \% = \frac{Loaded\ drug\ (mg)}{Total\ drug\ added\ (mg)}\ x\ 100$$

$$LC\ \% = \frac{Loaded\ drug\ (mg)}{Polymer\ (mg) + Loaded\ drug\ (mg)}\ x\ 100$$

1.2.2 Human serum incubation

In 1 mL Eppendorf tubes, 250 μL aliquots of a fresh sample of CUR loaded micelles were combined with 25 μL of human serum. The tubes were immersed in a water bath kept at 37 °C. The solutions were incubated for the indicated time intervals (0.5, 1, and 24 hours) and analyzed immediately by dynamic light scattering. Aliquots of the incubated samples were taken for electron microscopy studies.

1.2.3 Transmission Electron Microscopy (TEM)

The morphology of the nanoparticles (NPs) and protein corona formation were characterized using a Thermo Scientific Talos F200X G2 STEM operated at 200 kV located at the Facility for Electron Microscopy Research at McGill University. Samples were prepared by dropping a nanoparticle suspension (diluted 5x with MilliQ water) onto a glow discharged carbon film on a 200-mesh copper grid. The grid was then stained using a 2% uranyl acetate (UA) solution to enhance contrast. TEM images were acquired to determine nanoparticle size, shape, and to visualize the protein corona as a light-coloured amorphous layer surrounding the nanoparticles against a dark, electron-dense background. When indicated, samples were washed for removal of excess/unbound protein using a centrifugal filter unit (Millipore Sigma, Amicon® UFC5100) with molecular weight cutoff (MWCO) of 100kDa. In a typical experiment, 150 μL of serum incubated solution was added into the filtration apparatus and centrifuged at 7,500 rpm for 5 minutes. When 3 wash cycles were desired, 150 μL of PBS solution was added dropwise to the retentate and centrifugation was repeated. The latter step was repeated and the final retentate was re-diluted with 150 μL MilliQ water.

1.2.4 Drug release study (In the absence of human serum)

Freshly prepared CUR loaded micellar solutions were diluted 2x (final volume 2.0 mL) with PBS solution (pH 7.4). A hydrated Spectra/Por 3 dialysis membrane (standard RC, 3.5 kDa MWCO) underwent a final soak with PBS solution (pH 7.4) prior to transfer of the nanoparticle solution. The diluted micellar solution was transferred to the membrane and dialyzed against 140 mL of PBS solution (pH 7.4, containing 1% v/v Tween 80) at 37 ℃. At the specified time intervals, the membrane was briefly removed from solution, inverted 5x to homogenize, and aliquots (30 µL, triplicate) were taken from within the bag. Aliquots were diluted 40x with methanol and analyzed by UV-Vis. Release was calculated by changes in CUR absorbance at 422 nm.

1.2.5 Drug release study (In the presence of human serum)

Freshly prepared CUR loaded micellar solutions were diluted 2x (final volume 2.0 mL) with PBS solution (pH 7.4) before the dropwise addition of human serum (400 µL, 40% v/v with respect to 1 mL of micellar solution).
A hydrated Spectra/Por 3 dialysis membrane (standard RC, 3.5 kDa MWCO) underwent a final soak with PBS solution (pH 7.4). The nanoparticle/serum solution was allowed to stand 10 minutes before transfer to the dialysis membrane. Dialysis was carried out against 140 mL of PBS solution (pH 7.4, containing 1% v/v Tween 80) at 37 ℃. At the specified time intervals, the membrane was briefly removed from solution, inverted 5x to homogenize, and aliquots (30 µL, triplicate) were taken from within the bag.
In-bag release aliquots were diluted 40x with methanol and allowed to stand undisturbed in sealed vials for 4-6 hours at room temperature to facilitate complete protein precipitation. Then, samples were centrifuged at 4000 rpm for 10 minutes such that protein particles were pelleted out, enabling the supernatant to be readily decanted. CUR absorbance at 422 nm could then be accurately measured (without spectral distortion stemming from light scattering protein aggregates in methanol).

1.2.6 Critical Micelle Concentration

Critical micelle/aggregation concentrations were determined using pyrene as a fluorescence probe. Aliquots of a concentrated stock solution (20 µL, 198 µM in acetone) of pyrene were added to vials and allowed to dry over a period of 24 h under high air flow. Separately, a 2.0 mL micellar solution ([Polymer = 5 .0 mg/mL] was prepared and subsequently used to generate a total of 16 aqueous samples ranging from 1.0 mg/mL to 0.00025 mg/mL. Each solution (2.0 mL) was transferred to the vials containing known amounts of dried pyrene (final [pyrene] = 2.0 µM). The sealed vials were heated at 65 °C in a water bath for 3.0 h and then allowed to cool to room temperature overnight. Samples were measured after a 20 h. room temperature equilibrium period. Fluorescence excitation spectra were measured with a fixed emission wavelength of 390 nm. Intensity ratios (I_{337}/I_{334}) were plotted as a function of polymer concentration and the resulting curves fitted according to the Sigmoidal–Boltzmann equation.[2, 3] Critical micelle concentration, defined as the sigmoid center, was calculated using Excel Solver.

1.2.7 Binding Constant Determination (CUR – HSA)

A 2 mM stock solution of CUR was prepared in PBS buffer (pH 7.4) containing minimal methanol and used to titrate a 1.0 mL, 40 mg/mL PBS solution of human serum ([HSA] = 22 µM] in 10 µL increments. The intrinsic fluorescence of HSA was monitored over 300 – 450 nm with an excitation wavelength of 280 nm. The quenching of HSA fluorescence by CUR was used to monitor formation of the HSA-CUR complex according to the following modified Stern Volmer equation.

$$\log\left[\frac{F_0 - F}{F}\right] = \log K + n \log[CUR]$$

1.2.8 Encapsulated CUR Interaction with HSA

CUR-loaded nanocarriers were diluted 20x - 30x dropwise with pH 7.4 PBS buffer, and 1.0 mL of the resultant solution was transferred to a quartz cuvette. Serum solution was incrementally added to the cuvette and the mixture was homogenized. Fluorescence emission measurements were carried out at room temperature with selective CUR excitation (415 nm). Absorbance spectra were also obtained at each interval.

1.2.9 Free CUR Interaction with HSA

A stock solution of CUR (250 µg/mL, 679 µM) was prepared in methanol and subsequently slowly diluted 34x with pH 7.4 PBS. The resulting aqueous solution of CUR (20 µM) contained 1.5% methanol to ensure solubility. Separately, 56 µL of serum was added to a 2.0 mL aliquot of the CUR solution (final [HSA] = 30 µM) and allowed to rest for 10 minutes before analysis. Fluorescence emission measurements were carried out at room temperature with selective CUR excitation (415 nm).[4]

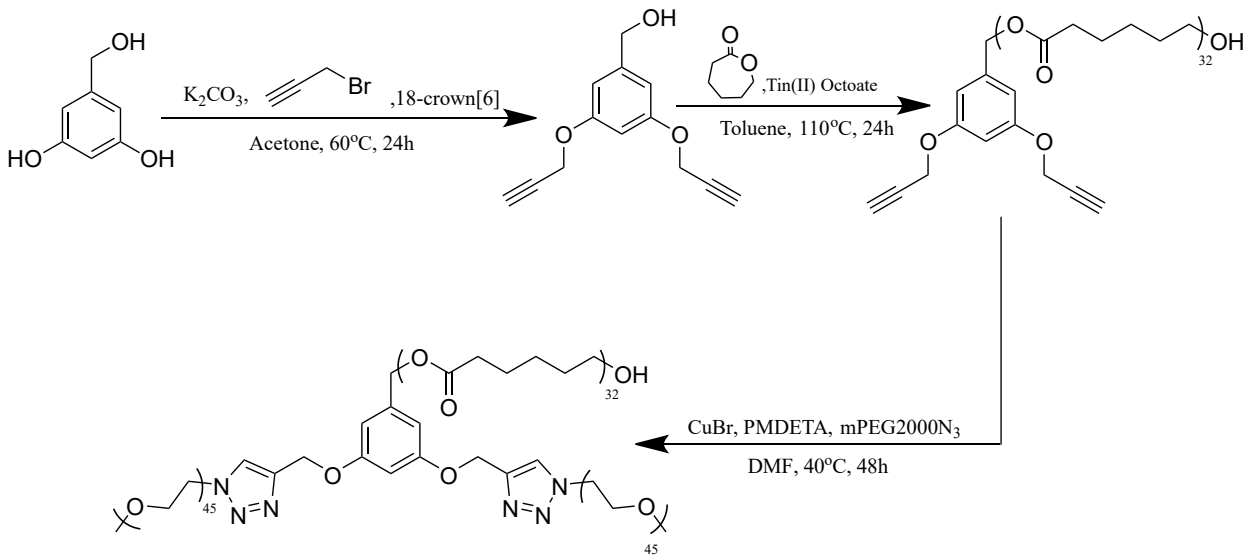

Scheme S.1 *Synthesis of miktoarm star polymer $(PEG_{45})_2$-b-PCL_{32}*

2. Synthesis and Structural Characterization

2.1 Synthetic Procedures and ^{1}H NMR Data

2.1.1 General procedure for the synthesis of miktoarm polymer

Di-propargylation was performed on commercial 3,5-dihydroxybenzyl alcohol according to literature procedure.[5] Ring opening polymerization of caprolactone employing the propargylated core as an initiator was carried out according to literature methodology.[6] Azide terminated polyethylene glycol monomethyl ether ($mPEG_{2000}$-N_3) was synthesized in two steps from commercially available monomethoxy polyethylene glycol 2000 (tosylation and subsequent azidation).[7,8] Copper (I) catalyzed alkyne-azide cycloaddition was performed according to literature procedure with modification.[9, 10]

^{1}H NMR (500 MHz, $CDCl_3$) δ 7.86 (s, 2H), 6.64 – 6.61 (m, 3H), 5.19 (s, 4H), 5.06 (s, 2H), 4.08 (t, *J* = 6.7 Hz, 62H), 3.72 – 3.58 (m, 398H), 3.40 (s, 6H), 2.33 (t, *J* = 7.5 Hz, 61H), 1.68 (m, 163H), 1.41 (m, 67H).
Degree of Polymerization: DP_{PCL}= $((I_{4.08} + I_{2.33} + I_{1.41}) / 6) / (I_{3.40} / 6) = 32$

2.1.2 Synthesis of linear diblock polymer

A dried three neck round bottom flask was charged with $mPEG_{2000}$ (2.64 g, mmol), distilled Ɛ-caprolactone (3.00 mL, mmol), and 20 mL dry toluene under a nitrogen atmosphere. The mixture was heated to 100 °C, at which time distilled and nitrogen purged Sn (II) ethyl hexanoate (0.10 mL,) was added via syringe. The solution was allowed to reflux at 105 °C for 18 hours under nitrogen. After cooling to room temperature, the solvent was removed under reduced pressure. The resulting oil was dissolved in 5 mL dichloromethane and dropped into a cooled mixture of diethyl ether (200 mL) and methanol (5 mL). The resulting precipitates were allowed to settle, collected by vacuum filtration, and dried under reduced pressure. The diblock copolymer (5.60 g) was obtained as a fine white powder.

^{1}H NMR (500 MHz, $CDCl_3$) δ 4.06 (t, *J* = 6.7 Hz, 61H), 3.64 (s, 222H), 3.38 (s, 3H), 2.30 (t, *J* = 7.5 Hz, 65H), 1.64 (m, 126H), 1.44 – 1.33 (m, 65H). DP_{PCL}= $((I_{4.06} + I_{2.30} + I_{1.44}) / 3) / (I_{3.38} / 3) = 32$

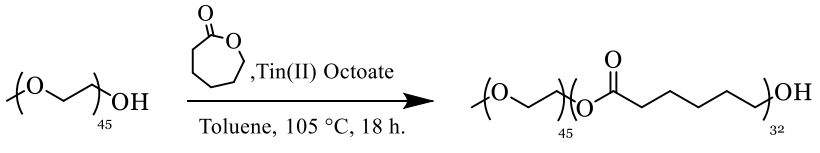

Scheme S.2 *Synthesis of diblock copolymer PEG_{45}-b-PCL_{32}*

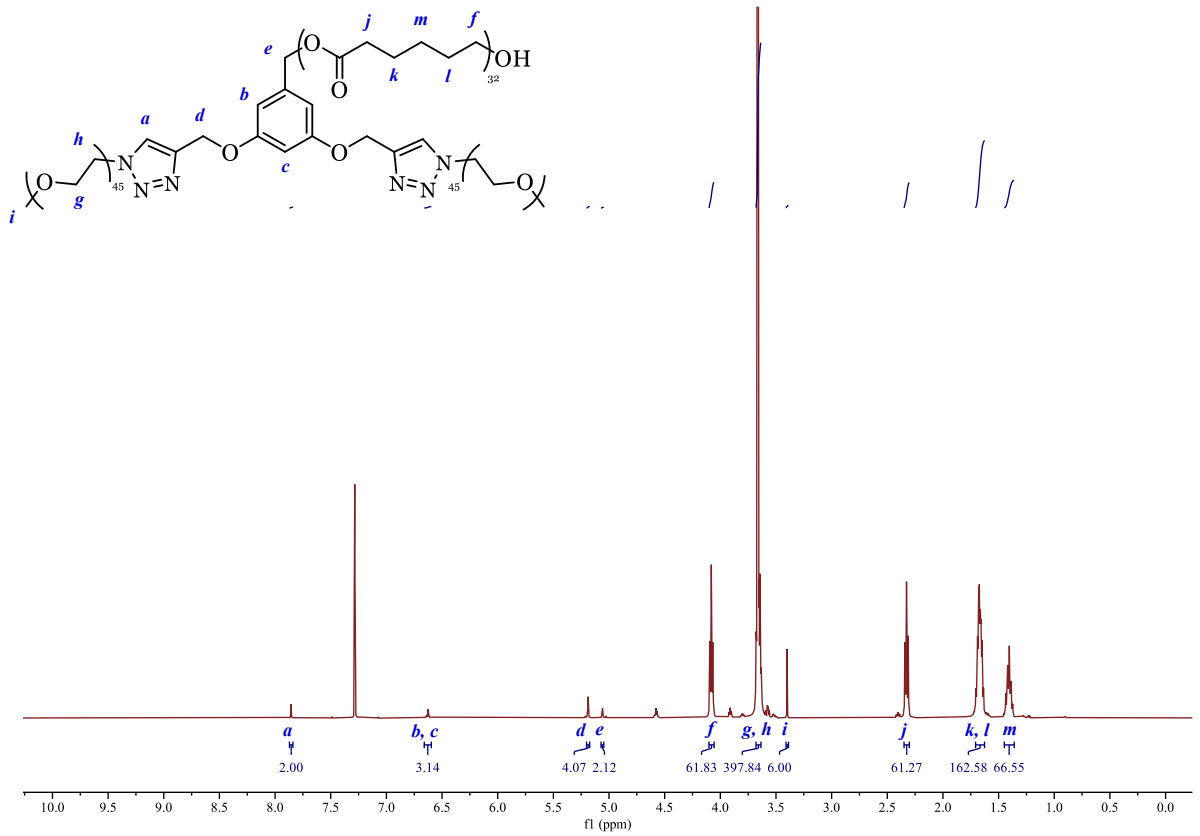

Figure S.1 *^{1}H NMR (500 MHz, $CDCl_3$) spectrum of miktoarm star polymer $(PEG_{45})_2$-b-PCL_{32}*

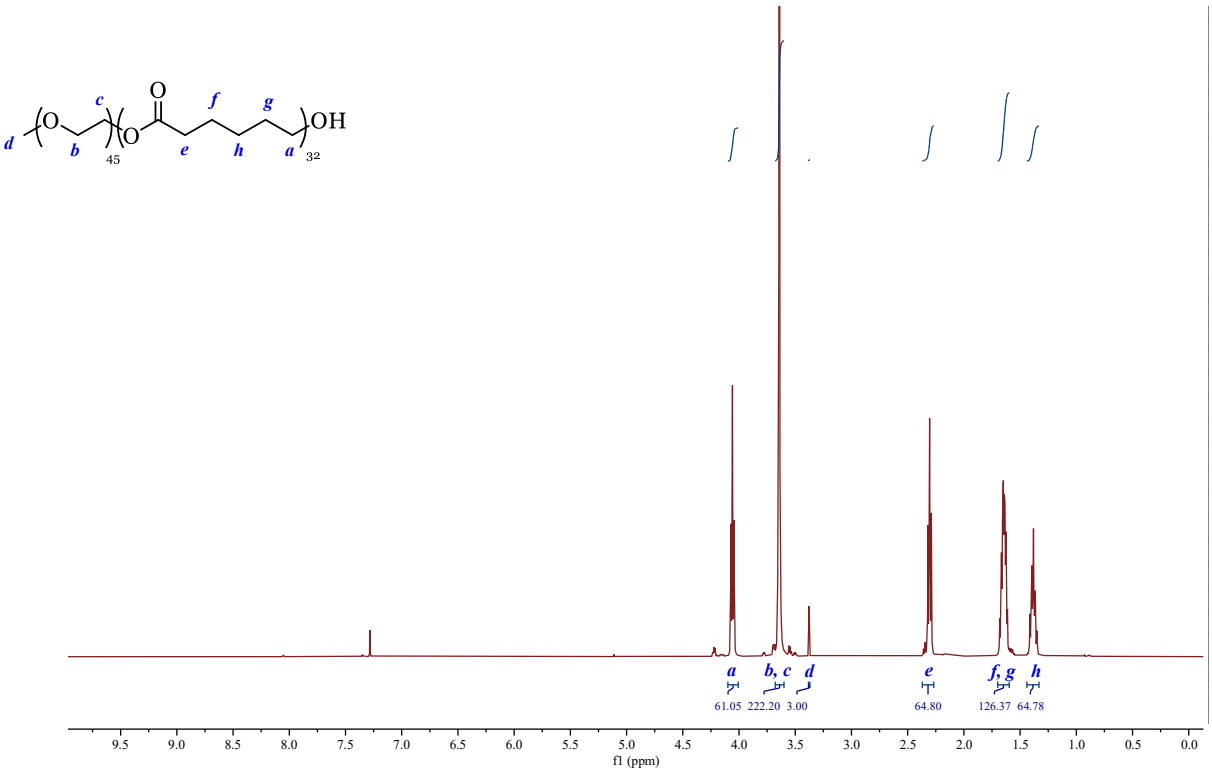

Figure S.2 *^{1}H-NMR (500 MHz, $CDCl_3$) spectrum of linear diblock polymer PEG_{45}-b-PCL_{32}*

2.2 Polymer and Nanoparticle Characterization

2.2.1 General

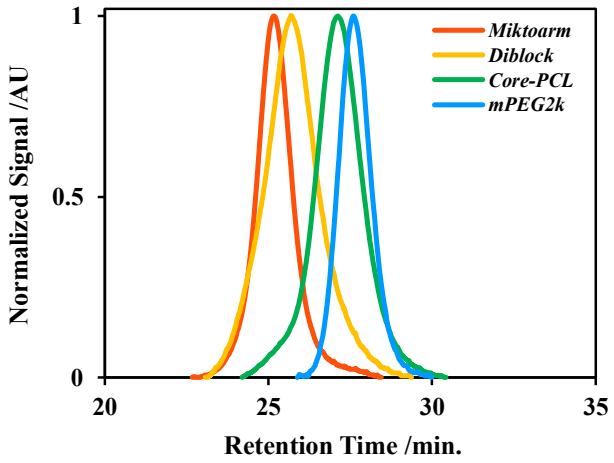

Figure S.3 *GPC chromatograms of miktoarm star polymer (R_T = 25.1 min, Đ = 1.11), precursor polycaprolactone (R_T = 27.1 min, Đ = 1.17), linear diblock copolymer (R_T = 25.7, Đ = 1.20) and $mPEG_{2000}$-N_3 (R_T = 27.6 min, Đ = 1.06)*

Polymer				Blank Micelles	
Sample	M_n [a]	Đ [b]	f_{PEG}	*Diameter /nm* [c]	Đ [d]
Diblock	5,600	1.20	0.36	35.9 ± 2.5	0.241 ± 0.025
Miktoarm	7,700	1.11	0.52	30.6 ± 0.4	0.191± 0.020

Table S.1 *Properties of diblock (AB) and miktoarm (AB_2) polymers and their blank nanoformulations. (a) Molecular weight calculated by ^1H NMR. (b) Polymer polydispersity by GPC. (c) Particle hydrodynamic diameter by DLS. (d) Polydispersity of nanoparticles by DLS. Parameters c/d reported as mean ± standard deviation of three separately prepared samples measured in triplicate*

Curcumin Loaded Micelles					
Sample	*CUR:Polymer* [a]	*Diameter /nm* [b]	Đ [c]	*EE %* [d]	*LC %* [d]
Diblock	1:10	24.7 ± 0.6	0.18 ± 0.04	89 ± 8	8.2 ± 0.7
Miktoarm	1:10	26.7 ± 0.3	0.23 ± 0.03	85 ± 5	8.0 ± 0.5

Table S.2 *Physical properties of CUR loaded nanoformulations of diblock (AB) and miktoarm (AB_2) polymers. (a) Feed ratio of drug (CUR) to polymer, by mass. (b) Hydrodynamic diameter by DLS. (c) Polydispersity of nanoparticles determined by DLS. (d) Encapsulation efficiency and loading capacity measured by UV-Vis. Parameters a-d reported as mean ± standard deviation of three separately prepared samples measured in triplicate*

2.2.2 Critical Aggregation Concentrations

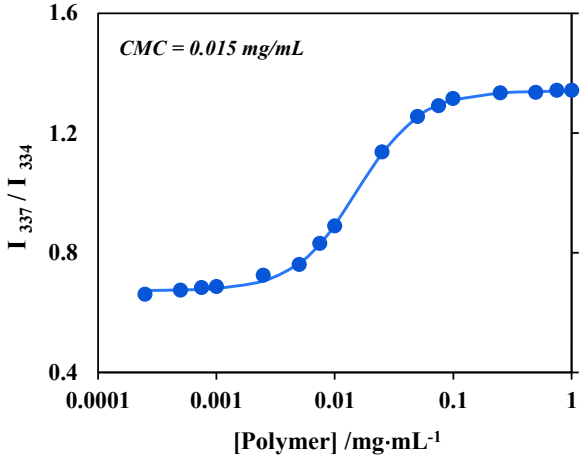

Figure S.4 *Critical micelle concentration determination for AB_2 miktoarm polymer*

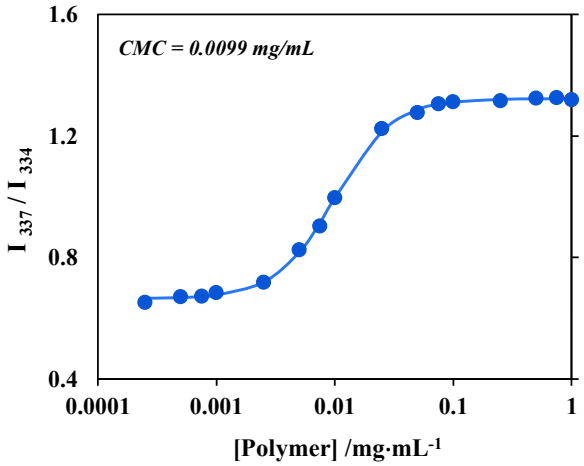

Figure S.5 *Critical micelle concentration determination for AB linear diblock polymer*

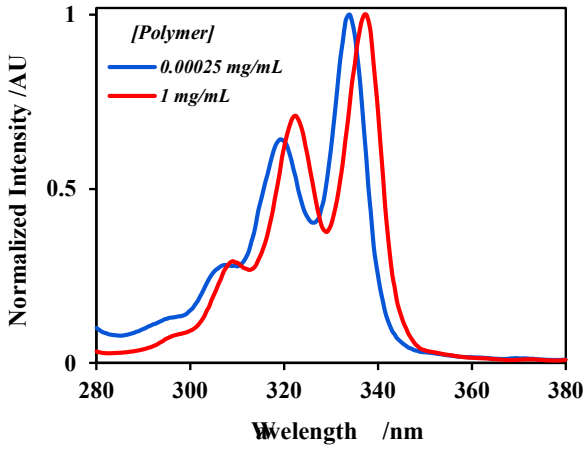

Figure S.6 *Normalized pyrene excitation spectra (λ_{em} = 390 nm) at miktoarm polymer concentrations 0.00025 mg/mL (< CMC) and 1.0 mg/mL (> CMC). Redshift of (0,0) band from 334 nm to 337 nm with transition from polar aqueous medium to non-polar micellar core environment.*

2.2.3 Nanoparticle PEG Density

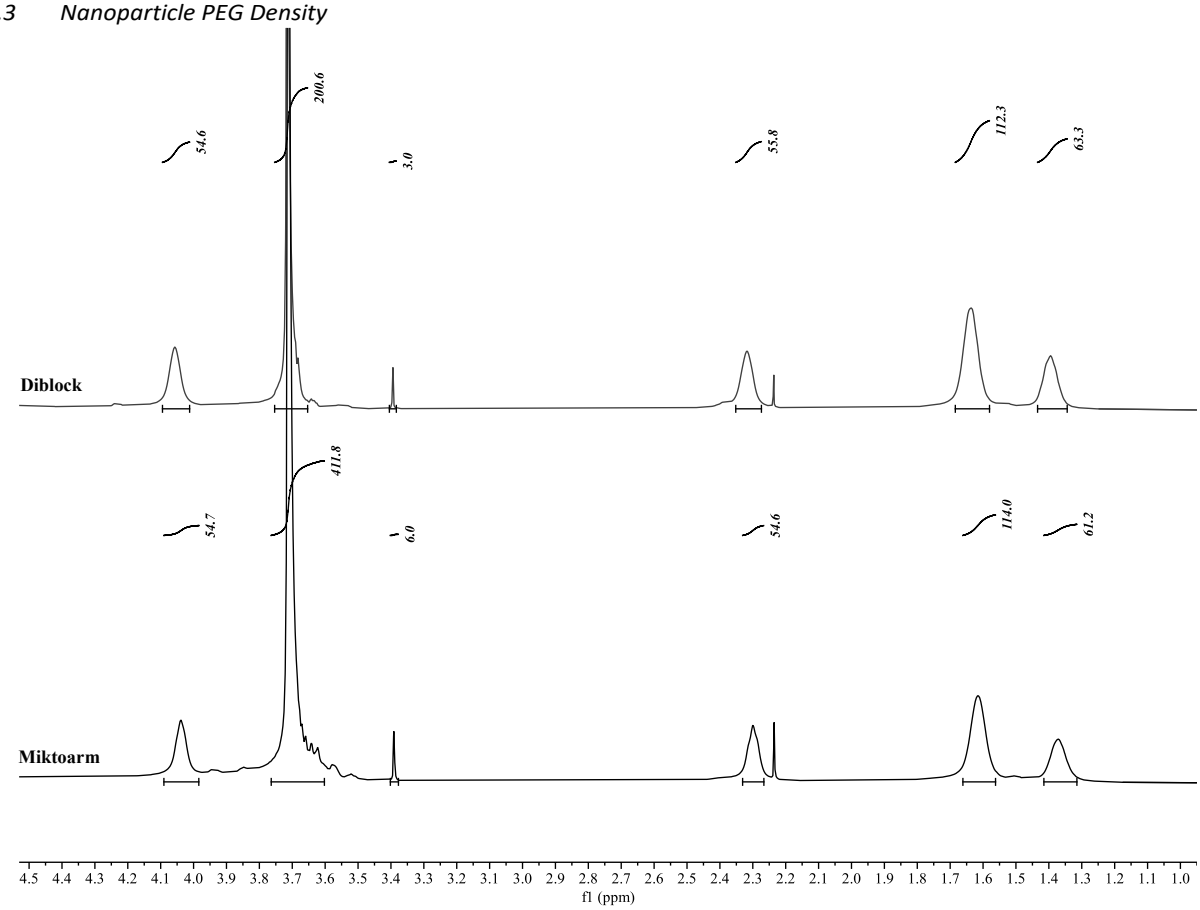

Fig S.7 *Stacked ^{1}H NMR spectra (500 MHz, D_2O) of self-assembled aqueous formulations of miktoarm and diblock polymers, illustrating differences in overall PEG content/surface density. Integration of broadened PCL peaks is constant between formulations while PEG integration doubles for micellar miktoarm solution. [Preparation: 10.0 mg of selected polymer dissolved in 100 µL of d_6-acetone, added dropwise to 500 µL of D_2O stirring at 400 rpm. Following evaporation of acetone (monitored by mass), solutions passed through 0.22 µm PVDF filter and transferred to NMR tube.]*

2.2.4 Release Kinetics

Model	Miktoarm (No serum)	Miktoarm (Serum)	Diblock (No serum)	Diblock (Serum)
Zero Order	$R^2 = 0.7313$	$R^2 = 0.2762$	$R^2 = 0.6249$	$R^2 = 0.5238$
First Order	$R^2 = 0.9571$	$R^2 = 0.8894$	$R^2 = 0.9323$	$R^2 = 0.9429$
Higuchi	$R^2 = 0.9935$	$R^2 = 0.9020$	$R^2 = 0.9831$	$R^2 = 0.9560$
Korsmeyer-Peppas	$R^2 = 0.9929$ n=0.495	$R^2 = 0.9751$ n= 0.357	$R^2 = 0.9893$ n = 0.447	$R^2 = 0.9716$ n= 0.420
Hixon-Cowell	$R^2 = 0.9241$	$R^2 = 0.8085$	$R^2 = 0.8907$	$R^2 = 0.8974$
Baker-Lonsdale	$R^2 = 0.9824$	$R^2 = 0.9869$	$R^2 = 0.9897$	$R^2 = 0.9869$
Weibull	$R^2 = 0.9991$ $\beta = 0.553$	$R^2 = 0.9991$ $\beta = 0.553$	$R^2 = 0.9894$ $\beta = 0.675$	$R^2 = 0.9987$ $\beta = 0.630$

Table S.3 *Kinetic modeling of CUR release from diblock (AB) and miktoarm (AB_2) nanoparticles with and without 40% (v/v) serum using DD solver.*

2.2.5 Serum Incubation – Sample Processing and Particle Visualization

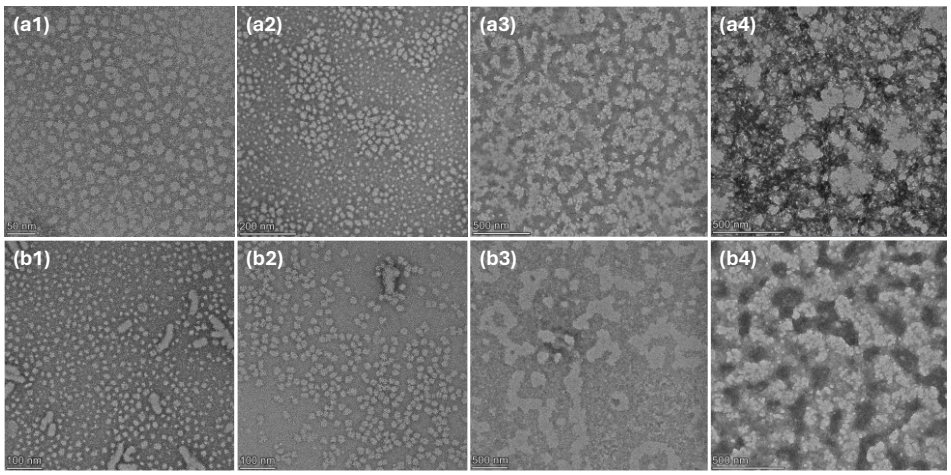

Figure S.8 *TEM images of diblock (AB) and miktoarm (AB_2) nanoparticles, stained with 2% uranyl acetate, showing morphology and post-serum protein corona (PC). (a1) Blank AB micelles: spherical, 22-35 nm dry size, ordered core-shell. (a2) CUR-loaded AB micelles: minor swelling, wider size range. (a3) Pre-wash serum AB NPs: less extensive amorphous PC, visible spheres on grey background. (a4) Post-wash (3 cycles) serum AB NPs: darker background confirming unbound protein removal. (b1) Blank AB_2 micelles: mostly spherical with worm-like aggregates. (b2) CUR-loaded AB_2 micelles: similar swelling and mixed morphologies. (b3) Pre-wash serum AB_2 NPs: denser PC obscuring boundaries. (b4) Post-wash (3 cycles) serum AB_2 NPs: patchy aggregates (~100 nm)*

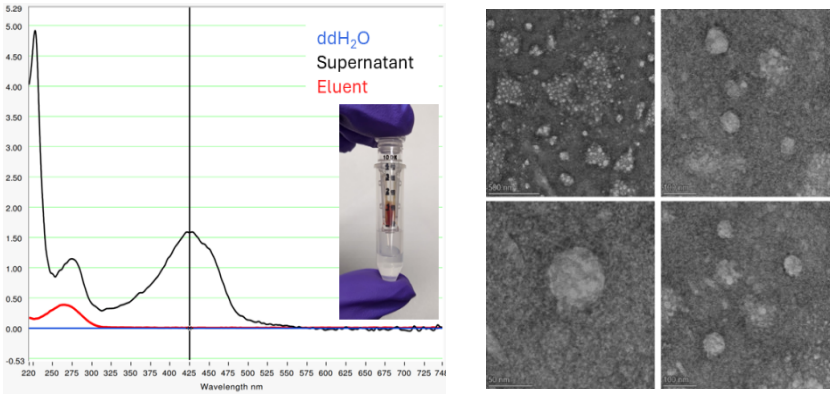

Fig S.9 *Confirmation of protein corona (PC) isolation on curcumin-loaded miktoarm (AB2) nanoparticles via centrifugal filtration (100 KDa MWCO) and visualization of adsorbed proteins.*
Left panel: UV-Vis absorbance spectra of the supernatant/retentate showing peaks at 425 nm (curcumin), ~280 nm, and ~230 nm (aromatic amino acids in bound serum proteins with minor contributions from curcumin/polymer core), and the eluent (passed fraction, transparent) displaying a broad peak at ~270 nm (unbound serum proteins, primarily HSA). Inset: Centrifugal filter unit (CFU), with the top compartment retaining yellow curcumin-loaded NPs with bound PC, while the bottom eluent is clear, confirming passage of free proteins (<100 kDa) and retention of NP-PC complexes (>100 kDa).
Right panel: Negative stained TEM image of washed AB_2 nanoparticles post-serum incubation at different magnification, revealing patchy surface structures indicative of adsorbed protein corona.

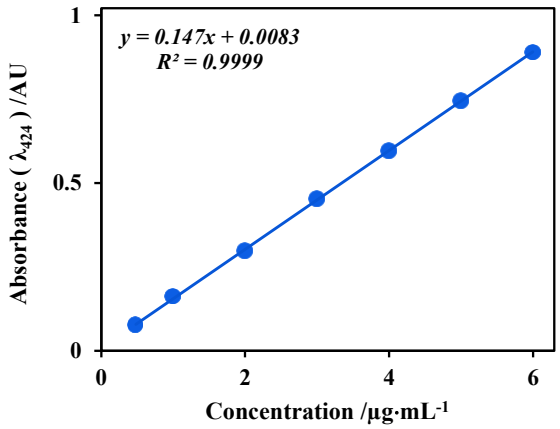

Fig S.10 *CUR calibration (2.5% PBS buffer in methanol) for calculation of encapsulation/loading parameters*

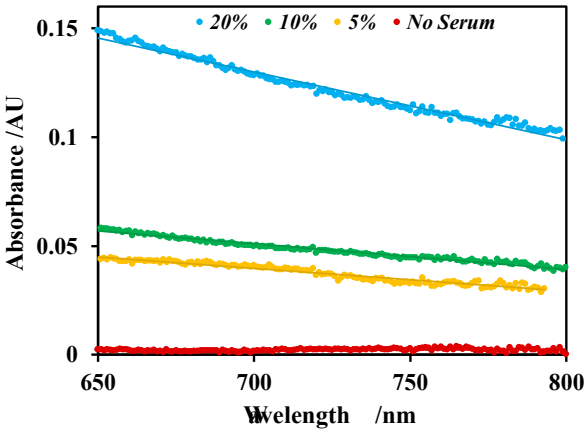

Fig S.11 *UV-Vis spectra of release aliquots showing baseline slope due to light scattering from protein precipitation upon methanol dilution (40x) at varying serum concentrations (v/v%). Long wavelength 'baseline' region in which CUR and HSA have non-detectable absorptivity (650-800 nm) is shown to highlight effect of protein precipitates.*

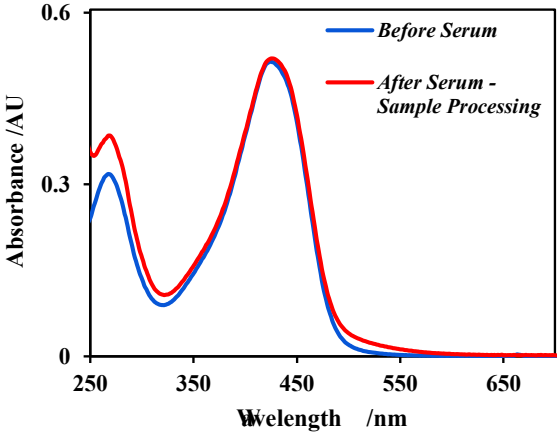

Fig S.12 *Comparison of spectra before serum addition and after precipitation-centrifugation processing, confirming negligible CUR loss and effective removal of scattering interference.*

3. Spectral and Photophysical Studies

3.1 Diblock Encapsulated CUR Emission – Serum Titration

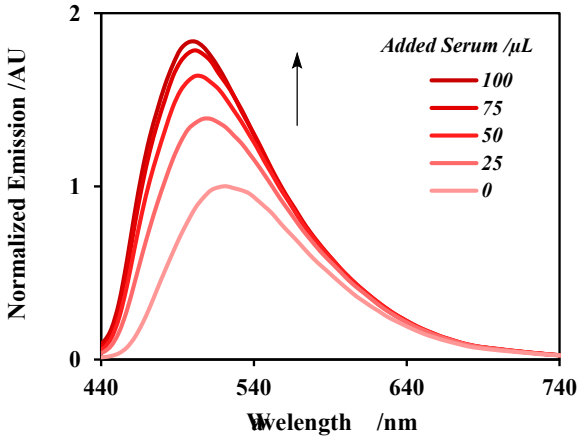

Figure S.13 *Fluorescence emission of CUR encapsulated in AB based nanoparticles (λ_{ex} = 415 nm, pH 7.4 PBS) with addition of human serum (Initial solution volume = 1.00 mL). Normalization sets initial (no serum) intensity to 1.*

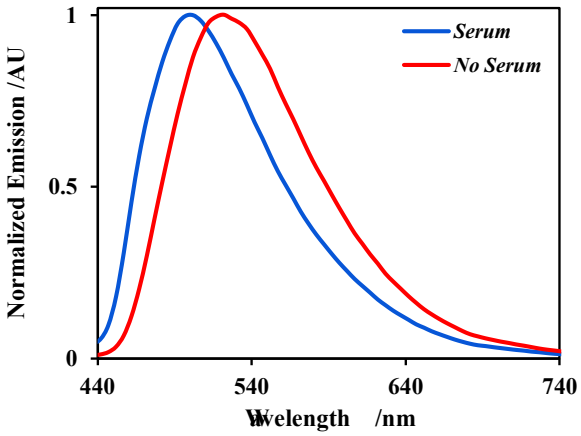

Figure S.14 *Normalized fluorescence emission of diblock encapsulated CUR (λ_{ex} = 415 nm, pH 7.4 PBS), before and after the addition of 100 µL of human serum.*

3.2 Encapsulated CUR Absorbance – Serum Titration

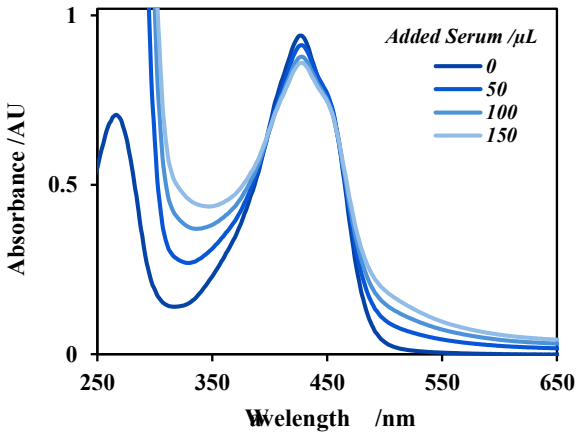

Figure S.15 *Absorbance spectra of miktoarm encapsulated CUR (pH 7.4 PBS) with successive addition of human serum (Initial solution volume = 1.00 mL).*

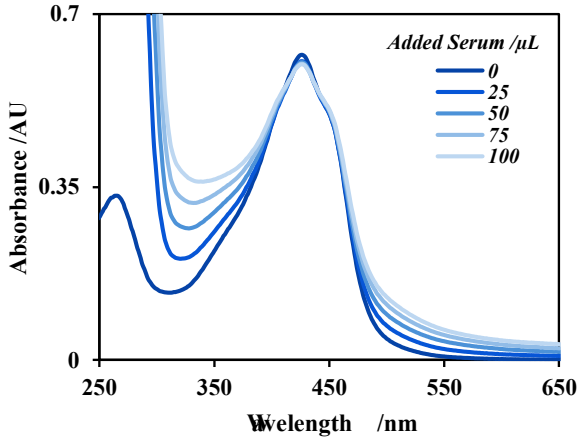

Figure S.16 *Absorbance spectra of diblock encapsulated CUR (pH 7.4 PBS) with successive addition of human serum product (Initial solution volume = 1.00 mL).*

3.3 Free CUR and CUR-HSA Complex Emission

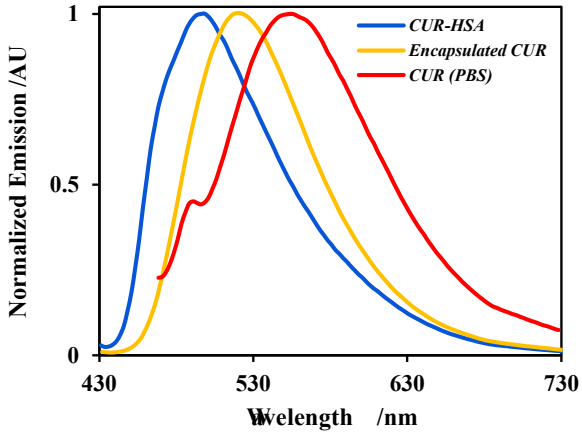

Figure S.17 *Normalized fluorescence emission of CUR-HSA complex, miktoarm encapsulated CUR, and CUR in aqueous solution (λ_{ex} = 415 nm, pH 7.4 PBS). Emission enhancement of aqueous CUR with serum addition (identical instrument settings): 15x.*

References

1. L. Painter, M. M. Harding and P. J. Beeby, Journal of the Chemical Society, Perkin Transactions 1, 1998, https://doi.org/10.1039/A803429J3041-3044.
2. G. Basu Ray, I. Chakraborty and S. P. Moulik, Journal of Colloid and Interface Science, 2006, 294, 248-254.
3. J. Aguiar, P. Carpena, J. A. Molina-Bolívar and C. Carnero Ruiz, Journal of Colloid and Interface Science, 2003, 258, 116-122.
4. A. Barik, K. I. Priyadarsini and H. Mohan, Photochemistry and Photobiology, 2003, 77, 597-603.
5. G. M. Soliman, R. Sharma, A. O. Choi, S. K. Varshney, F. M. Winnik, A. K. Kakkar and D. Maysinger, Biomaterials, 2010, 31, 8382-8392.
6. K. Khanna, S. Varshney and A. Kakkar, Macromolecules, 2010, 43, 5688-5698.
7. A. Hess, B. V. K. J. Schmidt and H. Schlaad, Polymer Chemistry, 2020, 11, 7677-7684.
8. H. Gao and K. Matyjaszewski, J Am Chem Soc, 2007, 129, 6633-6639.
9. M. Emami, R. Bikas, N. Noshiranzadeh, A. Kozakiewicz and T. Lis, ACS Omega, 2020, 5, 13344-13357.
10. Y. Chen, D. Liu, Q. Deng, X. He and X. Wang, Journal of Polymer Science Part A: Polymer Chemistry, 2006, 44, 3434-3443.